Synthesis of iron-based nanoparticles from ferrocene by femtosecond laser irradiation: Suppression of the particle growth in a mixture of water and hexane

Yuki Horikawa, Takuya Okamoto, Takahiro Nakamura, Yuhei O.Tahara, Makoto Miyata, Shingo Ikeda, Kenji Sakota, Tomoyuki Yatsuhashi

Citation	Chemical Physics Letters. 750; 137504
Issue Date	2020-07
Type	Journal Article
Textversion	Author
Highlights	◇ 界面活性剤の添加や遠心分離などの後処理なしで一定の粒子径に ◇ 原料濃度や反応時間によらず一定の粒子径に ◇ 混合溶液を用いる簡便な方法は様々なナノ粒子合成に適用できる
Rights	© 2020 Elsevier B.V. This manuscript version is made available under the CC-BY-NC-ND 4.0 License. http://creativecommons.org/licenses/by-nc-nd/4.0/. This is the accepted manuscript version.The formal published version is available at https://doi.org/10.1016/j.cplett.2020.137504.
DOI	10.1016/j.cplett.2020.137504
概要	添加剤や後処理が不要で、原料濃度や反応時間によらず大きさが一定の酸化鉄ナノ粒子の簡便な合成法の開発に成功しました。 酸化鉄ナノ粒子の合成には化学的手法が多く用いられてきました。しかし、粒径の制御に必要な界面活性剤などの添加剤が粒子の内部や表面に不純物として残留する可能性が問題視されてきました。そこで近年注目されているレーザーによる合成法を用い、水と有機溶媒の混合溶液を用いるだけで大きさが一定になる粒子の作製法を世界で初めて開発しました。 “添加剤も後処理も不要! 原料濃度や反応時間によらない大きさが一定の 酸化鉄ナノ粒子の簡便な合成法の開発に成功”. 大阪市立大学. https://www.osaka-cu.ac.jp/ja/news/2020/200422 (参照 2020-04-22)

Synthesis of iron-based nanoparticles from ferrocene by femtosecond laser irradiation: Suppression of the particle growth in a mixture of water and hexane

Yuki Horikawa,[a] Takuya Okamoto,[a] Takahiro Nakamura,[b] Yuhei O. Tahara,[a] Makoto Miyata,[a] Shingo Ikeda,[c] Kenji Sakota,[a] and Tomoyuki Yatsuhashi[a,*]

[a] *Graduate School of Science, Osaka City University, 3-3-138, Sugimoto, Sumiyoshi-ku, Osaka 558-8585, Japan*

[b] *Institute of Multidisciplinary Research for Advanced Materials, Tohoku University, 2-1-1 Katahira, Aoba-ku, Sendai 980-8577, Japan*

[c] *Osaka Research Institute of Industrial Science and Technology, 1-6-50 Morinomiya, Joto-ku, Osaka 536-8553, Japan*

*Corresponding author. E-mail address: tomo@sci.osaka-cu.ac.jp (T. Yatsuhashi)

ABSTRACT

Iron-based nanoparticles show unique magnetic properties, and their syntheses from metal complex solution by pulsed lasers have been widely studied; however, the aggregation of nanoparticles is unavoidable in homogeneous solution. We report the production of water-dispersible iron-based nanoparticles in a mixture of water and ferrocene *n*-hexane solution by femtosecond laser irradiation without using any additive agents. The mean diameter of iron-based nanoparticles (ca. 7 nm) is independent on the concentration of ferrocene or laser irradiation time. We propose that hexane microdroplets dispersed in water act as reaction vessels and reduce the opportunity of aggregation of primary nanoparticles.

Key words

laser-induced filaments, oil-in-water system, plasma, stirring

1. Introduction

The differences in physical and chemical properties of nanoparticles (NPs) compared with the bulk form make NPs important from both fundamental and applied scientific perspectives [1,2]. Large number of synthetic methods such as chemical synthesis, thermal decomposition, hydrothermal synthesis, and co-precipitation regarding the control of the size, shape, elemental composition, and dispersibility of NPs have been proposed [3]. Recently, laser-assisted syntheses of NPs have been increasingly recognized due to the possibility of producing NPs with various physical and chemical characteristics simply by varying laser irradiation conditions. Laser ablation in liquid (LAL), in which bulk materials are ablated in an inert solvent, is one of successful methods producing a variety of nanomaterials [4-7]. LAL is additive agent-free and non-contact production procedure under air atmosphere and at room temperature. The main focus of LAL has been noble metals [8], and LAL shows successful applications to a variety of materials such as organic crystals [9], inorganic materials [10-12], and transition metals [13-18].

Another laser-assisted synthesis of NPs is exposure of reactant solution to laser pulses. Focusing femtosecond (fs) laser pulses create a laser-induced plasma like a filament as a result of the balance between self-focusing by a nonlinear refractive index of medium and defocusing by plasma [19-21]. The laser intensity inside filaments is kept constant (ca. 10^{13} W cm^{-2} by intensity clamping) [22], and the density of electrons in laser-induced plasma in water reaches up to 10^{18} cm^{-3} [19]. It has been shown that using fs-laser pulses enables us to obtain noble metal NPs by the reduction of noble metal ions with strong reductants, solvated

electrons and hydrogen radicals [23,24], which are generated by multiphoton ionization and/or excitation of solvent [25]. This fs-laser induced nucleation method is a one-step process and does not require reducing agents or dispersants; however, it sometimes requires long-term laser irradiation to obtain small NPs in the absence of dispersants [26]. We recently succeeded synthesizing gold NPs with the diameter less than 10 nm from gold ions in a mixture of water and *n*-hexane in a short-time laser irradiation. We proposed that the adsorption of charged primary gold NPs on the surface of hexane microdroplets prevented NPs from growing [27]. The fs-laser induced nucleation is powerful method; however, the success is dependent on the reduction potential of metal ions: the more positive the reduction potential of metal ion, the more the metal ion tends to be reduced. Nevertheless, co-reduction and co-precipitation of several noble metal ions is possible due to the high-reduction power of solvated electrons. For example, solid-solution alloy NPs such as ternary alloy NPs (Rh-Pd-Pt) have been prepared from their metal ions since their reduction potentials are sufficiently high [28].

In contrast to noble metal ions, lanthanoid ions [29,30] and base metal ions [31,32], which have more negative reduction potential than noble metal ions, cannot be transformed to their metal NPs by fs-laser induced nucleation method since the reoxidation with dissolved oxygen does occur. Base metal NPs have been produced by the use of metal complexes instead of metal ions; however, the synthesized NPs were covered with carbons and/or contaminated by carbon agglomerates originating from organic solvent and ligands [33,34]. We reported the synthesis of carbon shell-free spherical iron-based NPs (Fe-based NPs) from ferrocene ($FeCp_2$) *n*-hexane solution by femtosecond near infrared laser pulses (0.8 μm, 40 fs) as well as by nanosecond ultraviolet laser pulses (355 nm, 8 ns) [35]. We propose that the use of aliphatic solvent such as *n*-hexane, which does not form carbon shell on NPs but decomposes into small fragments by fs-laser pulses, can provide bare Fe-based NPs. However,

unwanted carbon agglomerates originating from cyclopentadienyl ligands of $FeCp_2$ were formed in abundance. In addition, the mean diameter of Fe-based NPs obtained in $FeCp_2$ *n*-hexane solution was more than 10 nm. It is known that Fe-based NPs smaller than about 20 nm in diameter are expected to have superparamagnetic properties applicable to magnetic and biomedical materials [36]. We recently reported that the use of acetylacetonate complex in water resulted in the production of Fe-based NPs smaller than 10 nm without accompanying carbon agglomerates [37].

In this study, we use $FeCp_2$ in a mixture of water and *n*-hexane as a reactant. Water-dispersible iron-based NPs smaller than 10 nm in diameter regardless of the concentration of reactants and laser irradiation time are successfully produced without the aid of reductants, surfactant, capping agents, or centrifugation. Productions of Fe-based NPs from $FeCp_2$ in *n*-hexane with or without stirring were also performed. The possible mechanism about the suppression of particle growth in a mixture of water and *n*-hexane is discussed.

2. Experimental

Ferrocene ($FeCp_2$, Aldrich, 98%), *n*-hexane (Nacalai Tesque, spectral grade, ≥96.0%), and distilled water (Nacalai Tesque) were used without further purification. The mixture of 0.5 cm^3 water and 0.5 cm^3 $FeCp_2$ *n*-hexane solution (1.0×10^{-3} or 1.0×10^{-2} mol dm^{-3}) in a quartz cuvette with 1-cm optical path length was stirred with a crown-type PTFE-coated magnetic stirring bar. Femtosecond laser pulses (0.8 μm, 40 fs, 0.4 mJ, 1kHz) delivered from a Ti:Sapphire laser (Alpha 100/1000/XS hybrid; Thales Laser) were focused on the central part of the cuvette by using a planoconvex quartz lens with a focal length of 50 mm. For comparison purpose, 1.0 cm^3 $FeCp_2$ *n*-hexane solution (1.0×10^{-3} or 1.0×10^{-2} mol dm^{-3}) with or without stirring was also exposed to fs-laser pulses. Batch-type experiments were performed in all cases. Hereinafter, the $FeCp_2$ *n*-hexane solution is referred to as “the hexane

solution" and the mixture of water and $FeCp_2$ *n*-hexane solution as "the mixture". After the 5, 10, 15, or 20-min laser irradiation, 10 μL of the hexane solution or the water layer of the mixture was directly dropped onto a copper grid covered with amorphous carbon film (Nisshin EM). The drop was allowed to dry under air at room temperature to prepare specimens for transmission electron microscope (TEM) observations, which were performed with a JEOL JEM-1010 operated at 80 kV. Selected area electron diffraction (SAED) measurements were performed with a JEOL JEM-2100 operated at 160 kV. Measurements of energy dispersive X-ray spectra (EDS) were carried out by Topcon EM-002B operated at 200 kV. EDS mapping was performed by using FEI Titan^{TM} 80-300 in the STEM mode operated at 300 kV. The image of hexane microdroplets in water was taken by an inverted microscope (IX71, OLYMPUS) equipped with an objective (20×, OBL-20-A, Sigma Koki) and a CCD camera.

3. Results and discussion

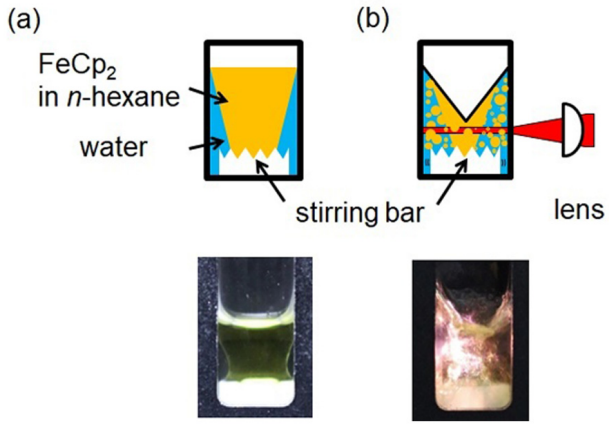

Fig. 1. (Top panel) schematic and (bottom panel) appearance of the mixture of water and $FeCp_2$ *n*-hexane solution (a) before and (b) during laser irradiation.

Fig. 1 shows the schematic and picture of the mixture of water and $FeCp_2$ *n*-hexane solution (the mixture) before and during laser irradiation. Violet-colored light was emitted

from laser-induced filaments during the laser irradiation. Scattering of light was significant due to the presence of bubbles, vortices, and microdroplets. Thus, we repeated batch-type experiments on different days to ensure the reproducibility of the experiments. The reproducibility of the production of NPs was judged by the similarity of the size distributions and the standard deviation of mean diameters. The mixing of solution resulted in the formation of hexane microdroplets, but they cannot be observed in situ. Therefore, we observed the hexane microdroplets in water by sampling the water phase after separating the mixture to two-phase solution by standing the cuvette. The diameter of hexane microdroplets was about 5.5 μm observed by using an optical microscope (Fig. 2).

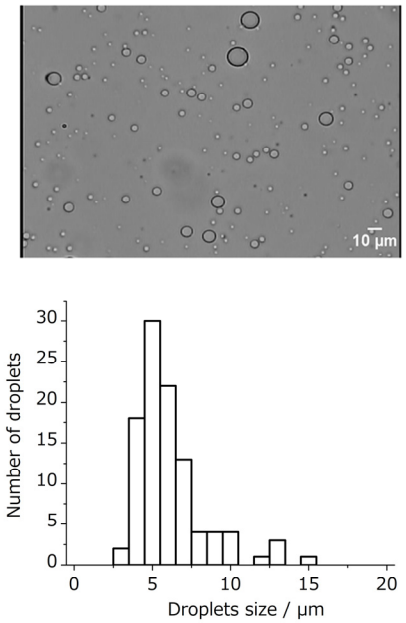

Fig. 2. (Top panel) optical microscope image and (bottom panel) size distribution of hexane microdroplets in water. The sample was collected from the water layer of the mixture of water and $FeCp_2$ *n*-hexane solution after the 10-min mixing. The concentration of $FeCp_2$ in *n*-hexane was 1.0×10^{-2} mol dm^{-3}. The mean diameter of the microdroplets was 5.5 μm. CV was 39.1%.

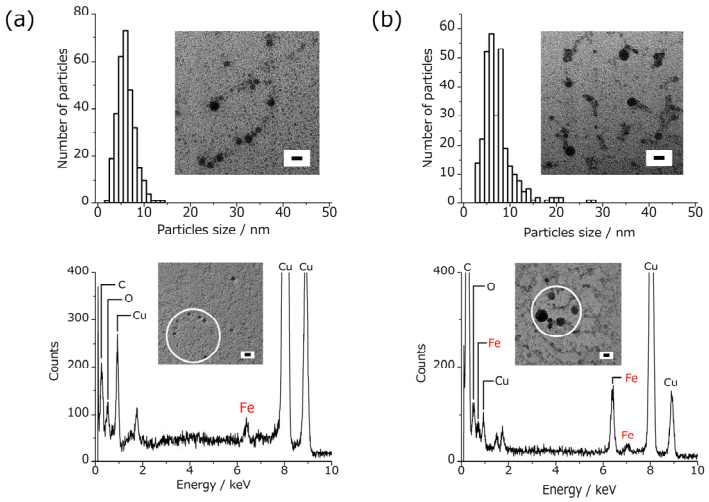

Fig. 3. (Top panel) size distributions, (bottom panel) EDS, and (insets) TEM images (scale bar: 10 nm) of Fe-based NPs collected from the water layer of the mixture of water and $FeCp_2$ *n*-hexane solution exposed to femtosecond laser pulses for 10 min. EDS were measured for the region indicated by white solid circle in the TEM image. The concentration of $FeCp_2$ in *n*-hexane was (a) 1.0×10^{-3} and (b) 1.0×10^{-2} mol dm^{-3}, respectively. The number of counted particles was 305.

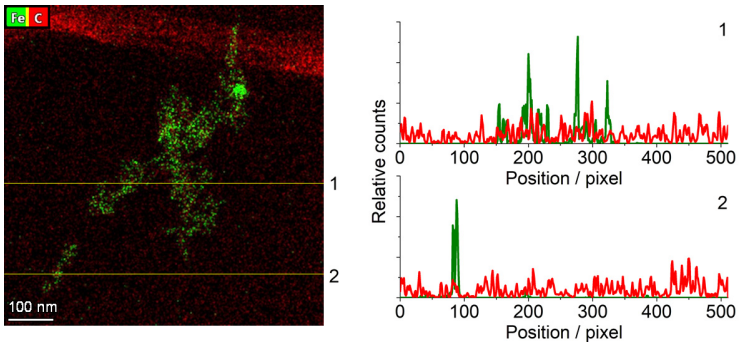

Fig. 4. (Left) Reconstructed EDS image of iron and carbon, and (right) elemental distributions on the lines 1 and 2 of the EDS image. Green and red represent iron and carbon, respectively. Fe-based NPs were collected from the water layer of the mixture of water and $FeCp_2$ *n*-hexane solution (1.0×10^{-2} mol dm^{-3}) exposed to femtosecond laser pulses for 20 min.

Fig. 3 shows size distributions, EDS, and TEM images of nanoparticles collected from the water layer of the mixture after the 10-min laser irradiation. It is emphasized that the nanoparticles with the mean diameter less than 10 nm were produced regardless of the concentration of $FeCp_2$ in *n*-hexane. The mean diameters of the spherical nanoparticles obtained in the water layer of the mixture of water and 1.0×10^{-3} and 1.0×10^{-2} mol dm^{-3} $FeCp_2$ *n*-hexane solution were 5.6 and 7.0 nm, respectively. The coefficient of variations (CVs), which equal to the standard deviations divided by mean diameters, obtained in the water layer of the mixture of water and 1.0×10^{-3} and 1.0×10^{-2} mol dm^{-3} $FeCp_2$ *n*-hexane solution were 34.4 and 50.4%, respectively. It is noted that small amounts of large particles (~30 nm) were formed when concentrated $FeCp_2$ solution was used. Carbon agglomerates were not observed in the water layer, but small amount of them can be found in the *n*-hexane layer of the mixture (Fig. S1 in the Supporting Information.) Fig. 4 shows the distribution of iron and carbon of the sample collected from the water layer of the mixture measured using carbon-covered grid with hydrophilic surface. It is better to use carbon-free grids for elemental analysis, but we cannot find particles using silicon- or germanium-covered grids with hydrophilic or hydrophobic surface probably because the affinity between particles and those grids is worse. Though the weak carbon signal, which is nearly back-ground level, originating from contaminants and carbon-coating on the grid surface appeared, it is evident that the distribution of iron and carbon was not coincided. Based on the results of elemental distributions, we conclude that obtained particles are not contaminated by carbons. Elemental mapping also indicated that the spherical nanoparticles were composed of iron and oxygen (Fig. S2 in the Supporting Information); however, the oxidation states of them were not identified. By analogy to the results obtained in *n*-hexane [35,37], the resultant nanoparticles would be consisted of oxidized irons. SAED analysis revealed that the resultant Fe-based NPs were amorphous states because only characteristic halo ring patterns were appeared.

Here we should mention that the iron-based NPs smaller than 10 nm in diameter were not dominant in the similar experiments using $FeCp_2$ dissolved in *n*-hexane (the hexane solution) as a reactant [35]. The growth of NPs should be related to many experimental parameters such as reactant concentration, stirring, solvent composition, and temperature as well as laser parameters. We fixed the laser parameters (wavelength, pulse duration, energy per pulse, chirp, repetition rate) and temperature for simplicity. In addition, only diluted (1.0×10^{-3} mol dm^{-3}) and concentrated (1.0×10^{-2} mol dm^{-3}) *n*-hexane solution of $FeCp_2$ were used. We compared the size distributions of Fe-based NPs obtained in the hexane solution (with or without stirring) with that obtained in the water layer of the mixture (with stirring) for different laser irradiation time. In addition, we also compared the relative abundance of large particles by introducing the index, P_L, which is the number of Fe-based NPs with the diameter between 15 and 50 nm relative to that of all Fe-based NPs.

Fig. 5 shows the size distribution of Fe-based NPs obtained by 10-min laser irradiation. The contribution of large particles indicated by dark color was significant for the Fe-based NPs obtained in the hexane solution, while that was almost absent for the Fe-based NPs obtained in the water layer of the mixture. Fig. 5 also compares mean diameter and P_L of Fe-based NPs. Those data are listed in Tables S1−S3 in the Supporting Information. In order to ensure the reproducibility of the experiments, we measured the size distributions of three different samples, which were obtained on different days. First, it should be emphasized that the mean diameters of Fe-based NPs obtained in the water layer of the mixture were independent on the concentration of $FeCp_2$ and laser irradiation time. Furthermore, P_L was significantly low compared with that obtained in the hexane solution. As for the hexane solution, the mean diameter and P_L of Fe-based NPs obtained in the concentrated solution were 1.3–1.9 and 1.5–6.5 times, respectively, higher than those obtained in the diluted solution. In the case of diluted solution, the mean diameter slightly decreased to ca. 90% by

20 min laser irradiation probably due to the fragmentation of NPs by successive fs-laser pulses, so-called laser fragmentation in liquid (LFL) [4]. Moreover, the mean diameter and P_L obtained in diluted solution decreased to 68–70% and 24–37%, respectively, by stirring. In contrast, the decrease of mean diameters and P_Ls by stirring was not observed in the concentrated solution. We conclude that it is not possible to reduce the mean diameter of Fe-based NPs down to 10 nm and achieve narrow size distribution even by long-term laser irradiation of diluted solution with stirring, if we use homogeneous hexane solution.

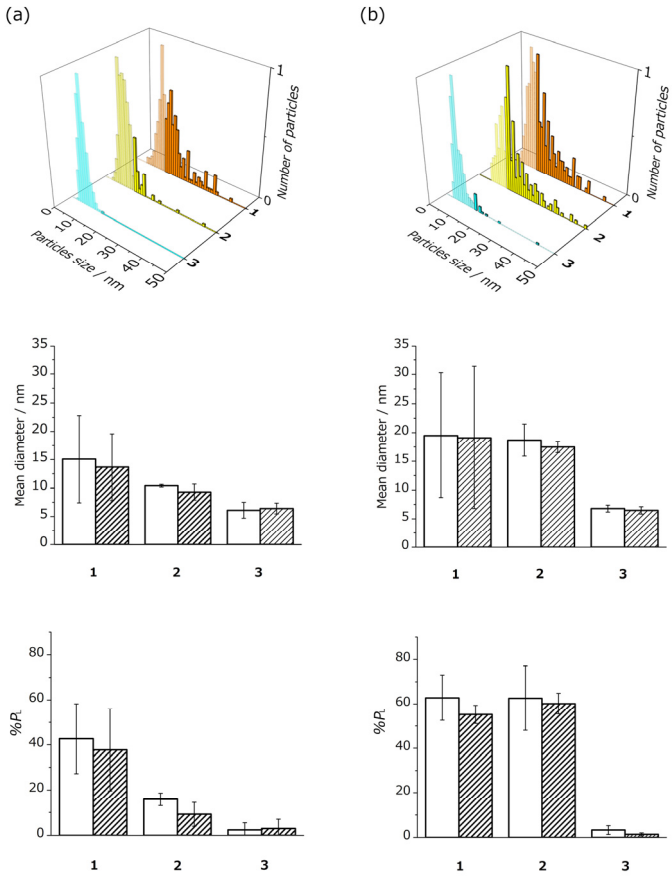

Fig. 5. (Top panel) size distribution, (middle panel) mean diameter, and (bottom panel) P_L of Fe-based NPs collected from (**1**) $FeCp_2$ *n*-hexane solution without stirring, (**2**) $FeCp_2$ *n*-hexane solution with stirring, and (**3**) the water layer of the mixture of water and $FeCp_2$ *n*-hexane solution. Size distributions displayed in the top panel were obtained for the sample exposed to laser pulses for 10 min. Mean diameter and P_L were obtained from the samples exposed to fs-laser pulses for 10 (open bars) and 20 min (cross-hatched bars). The vertical

bars give the standard deviation obtained in the three experimental runs carried out on different days. The concentration of $FeCp_2$ in *n*-hexane was (a) 1.0×10^{-3} and (b) 1.0×10^{-2} mol dm^{-3}, respectively. The data of mean diameter and P_L are listed in Tables S1−S3 in the Supporting Information.

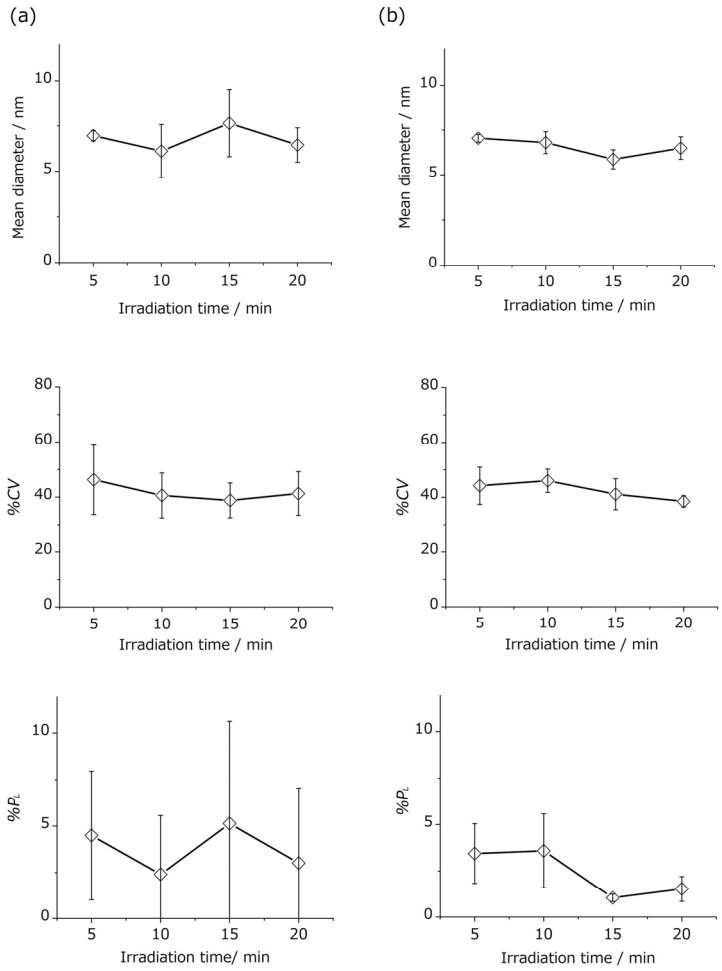

Fig. 6. (Top panel) mean diameter, (middle panel) CV, and (bottom panel) P_L of Fe-based NPs collected from the water layer of the mixture of water and $FeCp_2$ *n*-hexane solution as a function of laser irradiation time. The concentration of $FeCp_2$ in *n*-hexane was (a) 1.0×10^{-3} and (b) 1.0×10^{-2} mol dm^{-3}, respectively. The vertical bars give the standard deviation obtained in the three experimental runs carried out on different days. The data of mean diameter, CV, and P_L are listed in Tables S2 and S3 in the Supporting Information.

We further investigated the effect of laser irradiation time and concentration of $FeCp_2$ on the mean diameter, CV, and P_L of Fe-based NPs obtained in the water layer of the mixture (Fig. 6). Figure S3 in the Supporting Information shows typical TEM images. The data are listed in Tables S2 and S3 in the Supporting Information. The mean diameters and CVs of Fe-based NPs were nearly independent of laser irradiation time. Furthermore, they were insensitive to the concentration of $FeCp_2$. The effect of LFL by long-term laser irradiation on P_L might exist in the concentrated solution, whereas that in the diluted solution is uncertain because P_Ls were so scattered. Nevertheless, all these results suggest the advantages of using the mixture for the productions of Fe-based NPs with the mean dimeter less than 10 nm even with high concentration of reactant and by short-term laser irradiation.

We need to consider why the aggregation of primary Fe-based NPs is suppressed in the case of the mixture. We prepared hexane microdroplets containing $FeCp_2$ in water by mixing water and *n*-hexane. It should remind that $FeCp_2$ is dissolved only in *n*-hexane. Therefore, we can expect that hexane microdroplets act as small containers of reactants dispersed in water. Furthermore, the diameter of laser-induced filament is 10−100 μm [19,22]. Therefore, the photochemical reaction leading to the liberation of iron atoms take place only when hexane microdroplet containers are exposed to filaments. Supposing that nucleation and primary NPs production occur in a small part of a hexane microdroplet, the further aggregation forming large NPs might not occur unless the primary NPs in microdroplet are re-exposed to filaments. Fe-based NPs obtained in this study have another specific feature, that is water dispersibility. Fe-based NPs might earn water dispersibility presumably by the reactions with hydroxyl radicals produced in water during the laser irradiation [25,38]. Once Fe-based NPs escape from hexane microdroplets to bulk water, the probability of aggregation to form large particle is greatly decreased.

We propose the role of liquid-liquid interface in NP production: hexane microdroplets in water provide a confined volume for NP production and separate primary NPs each other. In the previous studies, we have shown other roles of liquid-liquid interface between water and organic solvent such as a diffusion-limiter and adsorption fields. The bilayer solution of water and organic solvent is a useful reaction environment to form hydrophilic or hydrophobic carbon nanoparticles (benzene/water) [38,39] , fluorine-rich hydrophilic carbon nanoparticles (hexafluorobenzene/water) [40], and low-chlorine carbon nanoparticles (dichloromethane/water) [41]. Those characteristic carbon nanoparticles are produced by utilizing the liquid–liquid interface that regulates the diffusion of organic molecules into water layer, where reactive species such as solvated electrons and hydroxyl radical are formed. The second role of liquid-liquid interface, namely adsorption effect, was demonstrated for the synthesis of single-nanometer-sized gold NPs: the aggregation of charged primary gold nanoparticles was suppressed by the adsorption of them on the surface of hexane microdroplets dispersed in water [27]. The proper use of liquid-liquid interface between water and organic solvent would be useful to produce desired NPs

4. Conclusion

We have synthesized Fe-based NPs (mean diameter ca. 7 nm) by exposing ferrocene in a mixture of water and *n*-hexane to femtosecond laser pulses. The size of Fe-based NPs was nearly independent on laser irradiation time or the concentration of ferrocene. We propose that the growth of nanoparticles is suppressed in a mixture of water and *n*-hexane because hexane microdroplets dispersed in water act as reaction vessels and reduce the opportunity of aggregation of primary nanoparticles. Fe-based NPs smaller than about 20 nm in diameter are expected to have superparamagnetic properties [36]. Such Fe-based NPs are promising materials for magnetic and biomedical applications [42] such as contrast agent of magnetic

resonance imaging [43], hyperthermia [44,45], and so on. We expect that synthesized Fe-based NPs hold a great promise for above-mentioned applications due to their size and water dispersible character [46]. Our strategy presented in this study can be utilized to synthesize nanoparticles of other metals, if corresponding metal complex is dissolved only in *n*-hexane.

Acknowledgements

The present research was supported in part by THE AMADA FOUNDATION Grant for Laser Processing Grant Number AF-2017224 to T. Y. We thank Mr. Kazuhiko Kondo of Thales Japan Inc. for his kind contribution to our laser system.

Conflict of interest

The authors declare that they have no known competing financial interests or personal relationships that could have appeared to influence the work reported in this paper.

Appendix A. Supplementary data

Supplementary data associated with this article can be found, in the online version, at doi:10.1016/j.cplett.

References

[1] M.C. Daniel, D. Astruc, Chem. Rev. 104 (2004) 293.

[2] C. Burda, X.B. Chen, R. Narayanan, M.A. El-Sayed, Chem. Rev. 105 (2005) 1025.

[3] B.L. Cushing, V.L. Kolesnichenko, C.J. O'Connor, Chem. Rev. 104 (2004) 3893.

[4] D.S. Zhang, B. Goekce, S. Barcikowski, Chem. Rev. 117 (2017) 3990.

[5] J. Xiao, P. Liu, C.X. Wang, G.W. Yang, Prog. Mater Sci. 87 (2017) 140.

[6] D.Z. Tan, S.F. Zhou, J.R. Qiu, N. Khusro, J. Photochem. Photobiol. C 17 (2013) 50.

[7] D. Amans, W.P. Cai, S. Barcikowski, Appl. Surf. Sci. 488 (2019) 445.

[8] S. Barcikowski, A. Hahn, A.V. Kabashin, B.N. Chichkov, Appl. Phys. A 87 (2007) 47.

[9] T. Asahi, T. Sugiyama, H. Masuhara, Acc. Chem. Res. 41 (2008) 1790.

[10] T. Tsuji, S. Sakaki, H. Fujiwara, H. Kikuchi, M. Tsuji, Y. Ishikawa, N. Koshizaki, J. Phys. Chem. C 122 (2018) 21659.

[11] H.H. Wang, O. Odawara, H. Wada, Appl. Surf. Sci. 425 (2017) 689.

[12] V. Amendola, S. Scaramuzza, F. Carraro, E. Cattaruzza, J. Colloid Interface Sci. 489 (2017) 18.

[13] A. Hu, J. Sanderson, Y. Zhou, W.W. Duley, Diamond Relat. Mater. 18 (2009) 999.

[14] X.Y. Chen, H. Cui, P. Liu, G.W. Yang, Chem. Mater. 20 (2008) 2035.

[15] A. De Bonis, T. Lovaglio, A. Galasso, A. Santagata, R. Teghil, Appl. Surf. Sci. 353 (2015) 433.

[16] V. Amendola, P. Riello, M. Meneghetti, J. Phys. Chem. C 115 (2011) 5140.

[17] B.K. Pandey, A.K. Shahi, J. Shah, R.K. Kotnala, R. Gopal, Appl. Surf. Sci. 289 (2014) 462.

[18] A. Kanitz, J.S. Hoppius, M.D.M. Sanz, M. Maicas, A. Ostendorf, E.L. Gurevich, ChemPhysChem 18 (2017) 1155.

[19] S.L. Chin, S.A. Hosseini, W. Liu, Q. Luo, F. Theberge, N. Akozbek, A. Becker, V.P. Kandidov, O.G. Kosareva, H. Schroeder, Can. J. Phys. 83 (2005) 863.

[20] A. Couairon, A. Mysyrowicz, Phys. Rep. 441 (2007) 47.

[21] L. Berge, S. Skupin, R. Nuter, J. Kasparian, J.P. Wolf, Rep. Prog. Phys. 70 (2007) 1633.

[22] C. Milian, A. Jarnac, Y. Brelet, V. Jukna, A. Houard, A. Mysyrowicz, A. Couairon, J. Opt. Soc. Am. B 31 (2014) 2829.

[23] B. Tangeysh, K.M. Tibbetts, J.H. Odhner, B.B. Wayland, R.J. Levis, Nano Lett. 15 (2015) 3377.

[24] L.M.F. Batista, V.K. Meader, K. Romero, K. Kunzler, F. Kabir, A. Bullock, K.M. Tibbetts, J. Phys. Chem. B 123 (2019) 7204.

[25] S.L. Chin, S. Lagace, Appl. Opt. 35 (1996) 907.

[26] T. Nakamura, Y. Herbani, D. Ursescu, R. Banici, R.V. Dabu, S. Sato, AIP Adv 3 (2013) 082101.

[27] T. Okamoto, T. Nakamura, K. Sakota, T. Yatsuhashi, Langmuir 35 (2019) 12123.

[28] M.S.I. Sarker, T. Nakamura, S. Sato, J. Nanopart. Res. 17 (2015) 259.

[29] D. Nishida, E. Yamade, M. Kusaba, T. Yatsuhashi, N. Nakashima, J. Phys. Chem. A 114 (2010) 5648.

[30] D. Nishida, M. Kusaba, T. Yatsuhashi, N. Nakashima, Chem. Phys. Lett. 465 (2008) 238.

[31] N. Nakashima, K. Yamanaka, M. Saeki, H. Ohba, S. Taniguchi, T. Yatsuhashi, J. Photochem. Photobiol., A 319 (2016) 70.

[32] N. Nakashima, K. Yamanaka, A. Itoh, T. Yatsuhashi, Chin J Phys 52 (2014) 504.

[33] Y. Liang, P. Liu, J. Xiao, H.B. Li, C.X. Wang, G.W. Yang, Sci.Rep. 3 (2013).

[34] A. Ouchi, T. Tsunoda, Z. Bastl, M. Marysko, V. Vorlicek, J. Bohacek, K. Vacek, J. Pola, J. Photochem. Photobiol., A 171 (2005) 251.

[35] T. Okamoto, T. Nakamura, R. Kihara, T. Asahi, K. Sakota, T. Yatsuhashi, ChemPhysChem 19 (2018) 2480.

[36] W. Li, J. Zaloga, Y.P. Ding, Y.F. Liu, C. Janko, M. Pischetsrieder, C. Alexiou, A.R. Boccaccini, Sci.Rep. 6 (2016) 23140.

[37] T. Okamoto, T. Nakamura, Y.O. Tahara, M. Miyata, K. Sakota, T. Yatsuhashi, Chem. Lett. 49 (2020) 75.

[38] T. Hamaguchi, T. Okamoto, K. Mitamura, K. Matsukawa, T. Yatsuhashi, Bull. Chem. Soc. Jpn. 88 (2015) 251.

[39] T. Yatsuhashi, N. Uchida, K. Nishikawa, Chem. Lett. 41 (2012) 722.

[40] T. Okamoto, K. Mitamura, T. Hamaguchi, K. Matsukawa, T. Yatsuhashi, ChemPhysChem 18 (2017) 1007.

[41] T. Okamoto, E. Miyasaka, K. Mitamura, K. Matsukawa, T. Yatsuhashi, J. Photochem. Photobiol., A 344 (2017) 178.

[42] S. Laurent, D. Forge, M. Port, A. Roch, C. Robic, L.V. Elst, R.N. Muller, Chem. Rev. 108 (2008) 2064.

[43] B.H. Kim, N. Lee, H. Kim, K. An, Y.I. Park, Y. Choi, K. Shin, Y. Lee, S.G. Kwon, H.B. Na, J.G. Park, T.Y. Ahn, Y.W. Kim, W.K. Moon, S.H. Choi, T. Hyeon, J. Am. Chem. Soc. 133 (2011) 12624.

[44] G. Kandasamy, A. Sudame, T. Luthra, K. Saini, D. Maity, ACS Omega 3 (2018) 3991.

[45] C.L. Dennis, A.J. Jackson, J.A. Borchers, P.J. Hoopes, R. Strawbridge, A.R. Foreman, J. van Lierop, C. Gruttner, R. Ivkov, Nanotechnology 20 (2009) 395103.

[46] A.K. Gupta, M. Gupta, Biomaterials 26 (2005) 3995.